ISSN 1063-7826, Semiconductors, 2013, Vol. 47, No. 4, pp. 574–578. © Pleiades Publishing, Ltd., 2013.
Original Russian Text © H.N. Mukhamedzyanov, V.F. Markov, L.N. Maskaeva, 2013, published in Fizika i Tekhnika Poluprovodnikov, 2013, Vol. 47, No. 4, pp. 557–562.

FABRICATION, TREATMENT, AND TESTING OF MATERIALS AND STRUCTURES

Study of the Characteristics of Photoresistors Based on Hydrochemically Deposited Films of $Pb_{0.902}Sn_{0.098}Se$ Solid Solution

H. N. Mukhamedzyanov^, V. F. Markov, and L. N. Maskaeva

Ural Federal University named after the first President of Russia B.N.Yeltsin, ul. Mira 19, Ekaterinburg, 620002 Russia

^e-mail: newage@isnet.ru

Submitted June 4, 2012; accepted for publication June 15, 2012

Abstract—Experimental samples of photoresistors based on a $Pb_{0.902}Sn_{0.098}Se$-solid solution semiconductor films obtained by the layer-by-layer deposition of individual selenides of lead and tin(II) with subsequent thermal activation are developed. The structure and morphology of the thin-film compositions $(SnSe–PbSe)_2$ are studied. The temperature dependences of the dark resistance, signal, noise and its ratio, as well as the frequency and spectral characteristics of photoresistors fabricated on the basis of $Pb_{0.902}Sn_{0.098}Se$ films in the range of 205–300 K are studied. The optimal bias voltages are determined. It is shown that the location of the maximum and the right boundary of the photoresponse for $Pb_{0.902}Sn_{0.098}Se$-based photoresistors is shifted, in comparison with PbSe, toward the long-wavelength region by 0.7 μm. The maximal detectivity of the studied photoresistors (2.0 × 2.0 mm) obtained at 230 K was 9×10^9 cm W^{-1} $Hz^{1/2}$. The advantages of using the $Pb_{0.902}Sn_{0.098}Se$-based photoresistors in the spectral range of 3.0–5.5 μm compared with PbSe-based ones are shown.

DOI: 10.1134/S1063782613040179

1. INTRODUCTION

The development of new photosensitive materials for the mid- and far-infrared (IR) ranges (3–14 μm) is a topical problem in the development of a modern infrared technique [1–5]. The CdHgTe-based and PbSnTe-based photodetectors, currently used in these ranges, are complex in fabrication and have unstable properties. Alternative materials are substitutional solid solutions in the lead selenide–tin(II) selenide system [6–8]. They exhibit inversion of the conduction bands upon formation of the overall PbSe–SnSe structure, which determines a decrease in the solid solution band gap with increasing SnSe content. This leads to a shift of the range of spectral sensitivity to the long-wavelength region of the IR spectrum [9, 10]. A promising method for obtaining PbSnSe solid solutions is the hydrochemical deposition method. It does not require complex manufacturing equipment and is well tested for obtaining PbSe layers [11–13]. In our previous studies, we determined the synthesis conditions of $Pb_{1-x}Sn_xSe$ films ($0 < x < 0.132$) by means of the joint [14] and layer-by-layer [15] hydrochemical deposition of individual selenides of lead and tin(II) with their subsequent thermal treatment in air. However, the photoelectric parameters of photoresistors (PR) fabricated based on them were not studied.

The goal of this study is to investigate the photoelectric, frequency, and spectral characteristics of photoresistors fabricated based on $Pb_{0.902}Sn_{0.098}Se$-solid solution films obtained by the layer-by-layer hydrochemical deposition of SnSe and PbSe with subsequent thermal treatment in air [16].

2. EXPERIMENTAL

The hydrochemical synthesis of SnSe and PbSe films was performed in sealed reactors 100 mL in volume made of molybdenum glass and placed into a U-10 thermostat with a temperature measurement accuracy of ±0.1%. As the substrate materials, we used the ST-50-1-2-grade glassceramic.

The PbSe films were obtained from a bath containing lead acetate, ethylene diamine, selenium carbamide, ammonium acetate, ammonium iodide and sodium sulfate. The synthesis temperature was 308 K and its duration was 60 min. To deposit the SnSe films, we used a reaction mixture prepared from tin(II) chloride, Trilon B, sodium hydroxide, selenium carbamide and sodium sulfate. The SnSe films were obtained at 343 K for 90 min. To form the films of $Pb_{1-x}Sn_xSe$ solid solutions, we sequentially deposited SnSe and PbSe layers with the obtainment of multilayer compositions. For their thermal treatment, we used a PM-1.0-7 furnace with temperature control accurate to ±2 K.

The film thickness was measured by the optical method using a Specord-75-IR spectrometer in the wavelength range of 2.5–25.0 μm.

The phase composition and structure of the films were studied by X-ray diffractometry using a DRON-3 diffractometer with copper radiation in the scanning mode with a step of 0.02° and a time of signal accumu-

lation at a point of 5 s. The SnSe fraction in the $Pb_{1-x}Sn_xSe$-solid solution structure was calculated by the Vegard rule [17] using the lattice constant of pseudocubic SnSe 0.6002 nm [18]. The error in determining the content of the substituting component in the solid solution was no larger than ±0.4 mol % with a confidence probability of 90%.

The photoelectric characteristics of the photoresistors (PR) were studied according to GOST (State Standard) 177892-79. To measure the volt–watt sensitivity and dark resistance, we used a K.54.410 measurement stand. The dimensions of the sensitiveelement of the studied samples were 2 × 2 mm. The time constant was measured by the two-frequency method accurate to ±10%.

Low-temperature studies of the photoelectric characteristics of the PRs were performed using a two-cascade thermoelectric cooler (TEC) in the temperature range 205–300 K with temperature control accurate to 0.2 K. As the TEC, we used a two-cascade cooler produced by the State Research-and-Production Enterprise of Thermophysical Instrument Making (GNIPP TFP) "Osterm" (St. Petersburg).

The relative spectral characteristics of the photoresistors were recorded using an SPM-2 double monochromator at a radiation modulation frequency of 1000 Hz.

The contact pads on the sensitive elements were formed by means of the electrochemical deposition of Ni. Gold conductors were soldered to the contact areas using a POSK low-temperature solder.

The photosensitive elements of the PR were mounted into a TO-5-type case or into a Burt case with the two-cascade TEC using a heat-conductive compound. The cases were filled with dry air.

As the input window in the uncooled PRs, we used sapphire glass (Al_2O_3) with a right transmission edge of 6.5 μm. The input window was glued into the top of the PR case using a special compound. The top was fixed onto the case via soldering or laser welding. As the input window in the cooled photoresistors, we used fluorite (CaF_2), which has a transmittance of up to 90% in the range 0.13–7.0 μm.

3. EXPERIMENTAL RESULTS AND DISCUSSION

When analyzing the X-ray diffraction patterns of our PbSe films, we identified only NaCl-type cubic structure ($B1$), which is characteristic of PbSe crystals. Comparison between the interplanar distances of the crystal lattice of the films and the reference data for PbSe single crystal showed that they almost coincide, which indicates a high degree of crystal-structure ordering.

In contrast to the PbSe films, the films of tin(II) selenide grow in a slower kinetic mode. Analysis of the X-ray diffraction patterns of tin(II) selenide shows that the films have a high degree of crystallinity, and the basic diffraction reflections correspond to the orthorhombic SnSe structure (the SnS type ($B29$), space group D_{2h}^{16}–P_{cmn}).

To attain the final goal, we obtained multilayer structures by means of the alternate deposition of PbSe and SnSe films. The number of layers of individual selenides was varied from two to eight. We synthesized and studied the following compositions: bilayer—SnSe–PbSe, three-layer—PbSe–SnSe–PbSe, four-layer—SnSe–PbSe–SnSe–PbSe, five-layer–PbSe–SnSe–PbSe–SnSe–PbSe, six-layer—SnSe–PbSe–SnSe–PbSe–SnSe–PbSe, and eight-layer—SnSe–PbSe–SnSe–PbSe–SnSe–PbSe–SnSe–PbSe. Their total thickness increased as the number of layers increased and constituted ~1.0 μm for the bilayer structures, 1.4–1.5 μm for the three-layer structures, 1.7–1.8 μm for the four-layer structures, 2.6–2.8 μm for the six-layer structures, and 3.4–3.6 μm for the eight-layer structures.

It follows from the results of X-ray studies of the synthesized structures that diffraction reflections correspond to the NaCl structure ($B1$) in all cases. It is established that the architecture of the PbSe film, which is the upper layer of the composition, differs from the individual PbSe deposited on the glass-ceramic substrate. For the four-layer structure, it is noted that crystallite sizes decrease compared with PbSe, namely, from 900–1200 nm to 200–300 nm, and to 30 nm according to the data of broadening the X-ray reflections. This fact can be interpreted from the viewpoint of varying the nucleus formation conditions for each subsequent PbSe layer. It should be noted that a decrease in the crystallite size should promote intensification of the diffusion processes between adjacent layers of metal selenides forming favorable potentialities for formation of the structure of the substitutional solid solution in the PbSe–SnSe system.

To sensitize these structures to infrared (IR) radiation, we used their thermal annealing in air in the temperature range 593–723 K. It was established that thermal treatment substantially changes the film morphology and composition.

It is important in principle that the diffraction reflections of the thermally treated multilayer compositions are shifted to the far-angle region, which is associated with the formation of $Pb_{1-x}Sn_xSe$ substitutional solid solutions ($0 \le x \le 0.132$). We also identified reflections from layers relating to the lead oxide and selenite phases (PbO, $PbSeO_3$) responsible for photosensitive properties. Our data on the thermal treatment of multilayer compositions allow us to make an important conclusion that various films have their own activation temperature, which characterizes their optimal degree of oxidation and the photoresponse level maximal for these conditions. As the number of layers increases, the photosensitivity maximum shifts

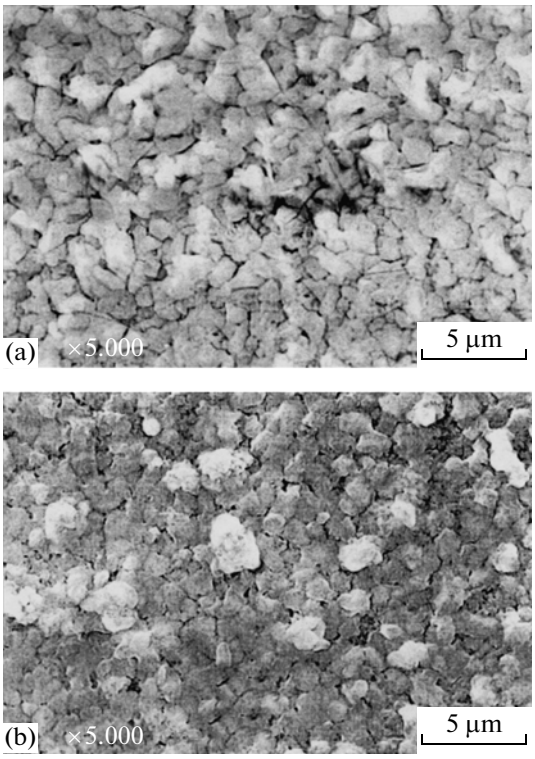

Fig. 1. Microphotographs of the (a) PbSe- and (b) $Pb_{0.902}Sn_{0.098}Se$-solid solution films. The treatment temperature is 643 K.

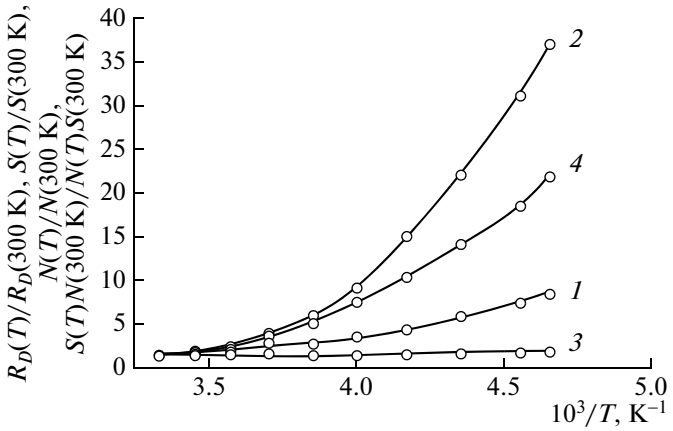

Fig. 2. Temperature dependences of the ratios of (*1*) the dark resistance $R_D(T)/R_D(300\ K)$, (*2*) the photoresponse signal $S(T)/S(300\ K)$, (*3*) noise $N(T)/N(300)$, and (*4*) the ratio $S(T)/N(300\ K)/N(T)S(300\ K)$ for the photoresistor based on the $Pb_{0.902}Sn_{0.098}Se$ solid solution.

to the region of higher activation temperatures. At the same time, as the number of layers increases, an increase in the nonuniformity of the crystallites in terms of sizes and composition is observed. The optimal variant is the synthesis of uniform four-layer compositions with subsequent thermal activation providing the formation of the $Pb_{0.902}Sn_{0.098}Se$ solid solution.

For comparison, Fig. 1 shows microphotographs of the thermally treated PbSe films (Fig. 1a) and the $Pb_{0.902}Sn_{0.098}Se$ solid solution (Fig. 1b) obtained from the four-layer composition $(SnSe–PbSe)_2$. It is seen from Fig. 1 that the microstructure of the films is different, namely, the average crystallite sizes in the case of solid solution formation are 220–300 nm against 770 nm for PbSe. We fabricated photosensitive elements for the PRs based on $Pb_{0.902}Sn_{0.098}Se$ layers.

In order to increase the photoresponse level, the compositions were thermally activated in an unsealed volume, which optimizes the oxidation kinetics of the films. For the four-layer composition, the maximal photosensitivity is attained at 634 K and a ratio of the medium volume in cm^3 to the area of the treated films in cm^2 of 32 [19].

Figure 2 shows the temperature dependences of the threshold parameters of the fabricated PRs, specifically, the dark resistance R_D, photoresponse signal S, and noise N in the temperature range 230–300 K. The mentioned parameters are presented in Fig. 2 relative to their values at 300 K: R_D (300 K), S (300 K), and N (300 K). Analysis of the dependences shows that upon cooling from 300 to 230 K, the dark resistance of the PR increases by a factor of approximately 8 (from 80–100 to 650–800 kΩ), the photoresponse signal increases by a factor of 38, while the noise increases only by a factor of 1.7. As a result, the signal/noise ratio and, consequently, the PR detectivity increases with cooling by a factor of almost 22, which offers their wide practical use. An important advantage of the PRs is also the small time constant, about 3 μs at 300 K.

In this study, we also investigated the dependence of the photoresponse signal of the PR based on the $Pb_{0.902}Sn_{0.098}Se$ solid solution on the modulation frequency f_m of the incident radiation flux from a blackbody of 573 K at 300 and 205 K (Fig. 3). The presented frequency characteristics show the fast response of the PR. It is seen from Fig. 3 that the PRs are able to operate without lowering the photoresponse signal at the modulation frequency of the incident radiation flux at 300 K to 30 kHz, and upon lowering the temperature to 205 K—to 5 kHz.

The dependence of the signal/noise ratio S/N on the applied voltage U presented in Fig. 4 made it possible to conclude that 24 V is the optimal bias voltage for the developed PRs. It is seen that upon varying (instability) the applied bias voltage within the limits ±5 V, the signal/noise ratio and, consequently, the PR detectivity are almost invariable.

The dependences of the detectivity D^* of the photoresistors based on PbSe and $Pb_{0.902}Sn_{0.098}Se$ films on the wavelength λ of the detected radiation for two different temperatures 230 and 300 K are shown in Fig. 5. Here, average values of the detectivity are presented for sampling of 100 photoresistors of each type. For the used solid solution, a substantial shift of the spec-

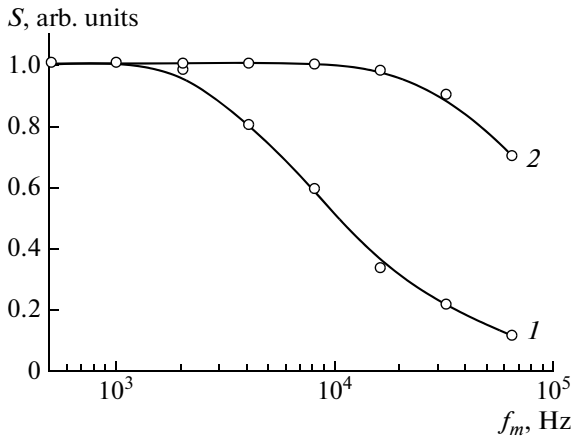

Fig. 3. Dependences of the photoresponse signal S of the photoresistor based on the $Pb_{0.902}Sn_{0.098}Se$ solid solution on the modulation frequency f_m of the optical flux at (*1*) 205 and (*2*) 300 K. The radiation source is a blackbody at 573 K. The bias voltage is 24 V.

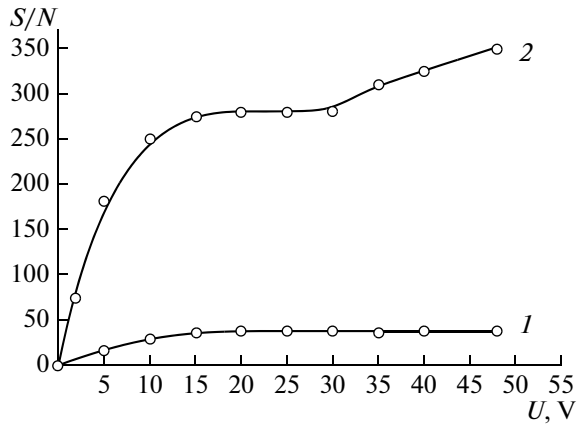

Fig. 4. Dependences of the signal/noise ratio S/N on the bias voltage U for a photoresistor based on the $Pb_{0.902}Sn_{0.098}Se$ solid solution at (*1*) 300 and (*2*) 230 K. The dimensions of the sensitive element are 2.0 × 2.0 mm.

tral characteristic of photosensitivity to the long-wavelength region is observed. It is seen from Fig. 5 that the location of the photosensitivity maximum of the PR based on the $Pb_{0.902}Sn_{0.098}Se$ solid solution is shifted compared with PbSe by 0.7 μm. In turn, the maximum of the spectral characteristic of photosensitivity in the range 300–230 K is shifted from 4.2 to 4.7 μm. The long-wavelength photosensitivity boundary of the $Pb_{0.902}Sn_{0.098}Se$ solid solution shifts from 5.5 to 6.0 μm in this case. From here, we can conclude that the optical band gap of the $Pb_{0.902}Sn_{0.098}Se$ solid solution changes from 0.225 to 0.207 eV, while for the PbSe film at 300 K, it is 0.248 eV. Greater cooling of the $Pb_{0.902}Sn_{0.098}Se$-based PR showed that at 80 K the right edge of the photoresponse at a level of 0.1 is located at a wavelength of 7.9–8.1 μm.

It should be noted that the maximal detectivity of the PRs $D^*(\lambda_{max})$ cooled to 230 K reached 9×10^9 cm W^{-1} $Hz^{1/2}$. The developed PRs are characterized by high stability of the parameters in time. For example, in the case of three years after casing, the signal decreased by only 5.8% on average, while the dark resistance increased by 10%.

The main characteristics of the PRs based on films of PbSe and the $Pb_{0.902}Sn_{0.098}Se$ solid solution obtained by means of the layer-by-layer deposition and subsequent thermal treatment of compositions of lead and tin(II) selenides are presented in the table.

Let us note the potentialities of using IR detectors based on the $Pb_{0.902}Sn_{0.098}Se$ solid solution compared with PbSe in photodetectors for an atmospheric transparency window of 3.0–5.5 μm. For example, one of the important practical tasks is timely determination of the initial stages of ignition and low-temperature sources of IR radiation involving these by means of the absorption band of carbon dioxide (4.3 μm). It is known [20] that a maximum in the emission spectrum of 4.02–4.18 μm and two low-intensity maxima 4.4 and 4.82 μm are distinguished in the spectrum of the flame "visible" through the atmosphere allowing for the absorption of carbon dioxide. The PbSe-based PR has lower detectivity in this wavelength range (no greater than 1×10^8 cm W^{-1} $Hz^{1/2}$. InSb-based PRs also require deep cooling to 77 K, which causes a considerable increase in their cost and a lowering of their operation reliability [21]. In this case, the prime cost of $Pb_{0.902}Sn_{0.098}Se$-based PRs insignificantly exceeds the cost of PbSe-based PRs when using the hydrochemical method for their fabrication.

Taking into account that the time constant of the developed experimental PRs based on the $Pb_{0.938}Sn_{0.062}Se$ film is higher by two orders of magnitude, while the sensitivity is higher than that of serial bolometers used in systems of railroad automation of temperature controlling of axle boxes of wheel pairs by

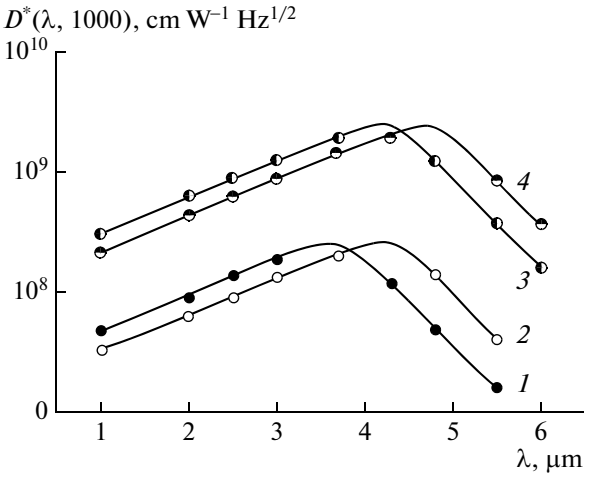

Fig. 5. Dependences of the detectivity D^* of the photoresistors (average values) based on (*1*, *3*) PbSe films and (*2*, *4*) $Pb_{0.902}Sn_{0.098}Se$ films on the wavelength λ at (*1*, *2*) 300 and (*3*, *4*) 230 K.

Photoelectric parameters of photodetectors based on PbSe and $Pb_{0.902}Sn_{0.098}Se$ films obtained by the technology of layer-by-layer deposition

Photoelectric parameters	Layer material			
	PbSe		$Pb_{0.902}Sn_{0.098}Se$	
	Temperature, K			
	300	230	300	230
Spectral range, μm	0.6–4.5	0.6–5.5	1.0–5.5	1.0–6.0
λ_{max}, μm	3.6 ± 0.1	4.1 ± 0.1	4.3 ± 0.2	4.8 ± 0.2
Detectivity $D^*(\lambda_{max}; 1000)$, cm W^{-1} $Hz^{1/2}$	$(2–6) \times 10^9$	$(3–9) \times 10^9$	$(2–6) \times 10^9$	$(3–9) \times 10^9$
Volt–watt sensitivity, V/W	$(2–6) \times 10^2$	$(6–11) \times 10^2$	$(2–6) \times 10^2$	$(6–11) \times 10^2$
Time constant τ, μs	3–5	30–40	2–4	12–30
Dark resistance, kΩ/square	150–400	250–800	60–300	200–800
Bias voltage, V	24	24	24	24
Dimensions of the sensitive element, mm	2.0 × 2.0	2.0 × 2.0	2.0 × 2.0	2.0 × 2.0
Input-window material	Sapphire	Sapphire	Fluorite	Fluorite

a factor of 4 [22]. Their use will allow an increase in the motion velocity of trains at linear control points.

4. CONCLUSIONS

We developed and fabricated experimental samples of uncooled and cooled single-element photoresistors sensitive in the IR spectral region (1.0–6.0 μm) based on films of the $Pb_{0.902}Sn_{0.098}Se$ solid solution obtained by the layer-by-layer hydrochemical deposition of PbSe and SnSe with subsequent thermal activation.

The PRs developed based on the $Pb_{0.902}Sn_{0.098}Se$-solid solution film possess a dark resistance of 80–800 kΩ and a detectivity $D^*(\lambda_{max}; 1000)$ of up to 9×10^9 cm W^{-1} $Hz^{1/2}$ in a range of photosensitive-element working temperatures of 230–300 K; they are characterized by a fast response permitting operation without lowering the photoresponse signal at a modulation frequency of the incident radiation flux of up to 30 kHz at 300 K and up to 5 kHz at 205 K.

The PRs based on the $Pb_{0.902}Sn_{0.098}Se$ solid solution have substantial advantages compared with the PbSe-based ones for the solution of some practical issues in the spectral range of 3.0–5.5 μm.

REFERENCES

1. *Optical and Infrared Detectors*, 2nd ed., Ed. by R. J. Keyes (Springer-Verlag, New York, 1980; Radio i svyaz', Moscow, 1985).
2. G. Gaussorgues, *Infrared Thermography* (Springer, 1994; Mir, Moscow, 1988).
3. B. N. Formozov, *Aerospace Photosensors in Visual and Infrared Ranges* (St.-Petersburg, GUAP, 2002) [in Russian].
4. L. N. Kurbatov, Prikl. Fiz., No. 3, 5 (1999).
5. A. M. Yushin, *Optoelectronic Devices and their Foreign Analogs*, The Handbook (IP Radiosoft, Moscow, 2000) [in Russian].
6. B. A. Volkov, O. A. Pankratov, and A. V. Sazonov, Sov. Phys. Solid State **26**, 255 (1984).
7. V. S. Zemskov and V. B. Lazarev, *Solid Solutions in Semiconductor Systems*, the Handbook (Nauka, Moscow, 1978) [in Russian].
8. N. P. Gavaleshko, P. N. Gorlei, and V. A. Shenderovskii, *Narrow-Band Semiconductors: Production and Physical Properties* (Nauk. Dumka, Kiev, 1984) [in Russian].
9. A. Szczerbakow and J. Berger, J. Cryst. Growth **139**, 172 (1994).
10. A. V. Sazonov, Extended Abstract of Candidate's Dissertation (Moscow, 1984).
11. H. N. Mukhamedzyanov, M. P. Mironov, S. I. Yagodin, L. N. Maskaeva, and V. F. Markov, Tsvetn. Met. **12**, 57 (2009).
12. N. A. Tret'yakova, V. F. Markov, L. N. Maskaeva, and H. N. Mukhamedzyanov, Kondens. Sredy Mezhfaz. Granitsy **7**, 189 (2005).
13. V. F. Markov, M. P. Mironov, S. V. Brezhnev, and L. N. Maskaeva, Butler. Soobshch. **17** (6), 22 (2000).
14. N. A. Tret'yakova, V. F. Markov, M. P. Mironov, V. F. D'yakov, and L. N. Maskaeva, Khim. Khim. Tekhnol. **51** (7), 37 (2008).
15. M. P. Mironov, A. Yu. Kirsanov, V. F. D'yakov, L. N. Maskaeva, and V. F. Markov, Butler. Soobshch. **19** (3), 45 (2010).
16. V. F. Markov, H. N. Mukhamedzyanov, L. N. Maskaeva, and Z. I. Smirnova, Semiconductors **45**, 1404 (2011).
17. L. Vegard, Z. Phys. **5**, 17 (1921).
18. *ASTM X-Ray Diffraction Date Cards* (Phyladelphia, 14–159, 1968).
19. M. P. Mironov, V. F. Markov, L. N. Maskaeva, V. F. D'yakov, R. D. Mukhamed'yarov, H. N. Mukhamedzyanov, and Z. I. Smirnova, RF Patent No. 2357321 (15) MZhGN01L21/36, Byull. No. 15 (2009).
20. V. V. Tarasov and Yu. G. Yakushenkov, *Staring-Type Infrared Systems* (Logos, Moscow, 2004) [in Russian].
21. Ya. P. Salii, Semiconductors **40**, 172 (2006).
22. V. F. D'yakov, M. P. Mironov, R. D. Mukhamed'yarov, H. N. Mukhamedzyanov, V. F. Markov, and L. N. Maskaeva, Transport Urala **21** (2), 94 (2009).

Translated by N. Korovin